Consolidation considering clogging effect under uneven strain assumption

Sijie Liu[1], Yuanqiang Cai[2], Honglei Sun[3], Xueyu Geng[4], Li Shi[5], Xiaodong Pan[6]

Abstract

In land reclamation projects, the vacuum preloading method is widely used to strengthen dredged fills by removing water. However, during the improvement process clogging inevitably occurs in the drains and soils, hindering the water drainage and causing inhomogeneous consolidation results. Therefore, it is essential to evaluate the effect of clogging on the consolidation behavior of dredged slurry at different radii. In this study, analytical solutions are derived under an uneven strain assumption to calculate the consolidation in the clogging zone and the normal zone, with time-dependent discharge capacity and clogging in the soil considered. Results calculated by the proposed solutions indicate that the clogging effect slows down the development of consolidation, reduces the final consolidation degree, and increases the difference between consolidations at different radii. It is found that the clogging effect's influence varies with the speed of the discharge capacity decay, the value of the initial discharge capacity of the drain, the permeability, and the radius of the clogging zone. Finally, a practical application of the proposed solution is discussed, and the proposed solution is suggested in the calculation of consolidation when treating high-water-content slurry.

Keywords: clogging, consolidation, dredged slurry, uneven strain, vacuum preloading

[1]Ph.D. Candidate, Research Center of Coastal and Urban Geotechnical Engineering, College of Civil Engineering and Architecture, Zhejiang University, Hangzhou 310058, P.R. China. Email: liusijie@zju.edu.cn
[2]Professor, Research Center of Coastal and Urban Geotechnical Engineering, College of Civil Engineering and Architecture, Zhejiang University, Hangzhou 310058, P.R. China; Professor, Institute of Geotechnical Engineering, College of Civil Engineering, Zhejiang University of Technology, Hangzhou 310000, P.R. China. Email: caiyq@zju.edu.cn
[3]Professor, Institute of Geotechnical Engineering, College of Civil Engineering, Zhejiang University of Technology, Hangzhou 310000, P.R. China. Email: sunhonglei@zju.edu.cn (corresponding author)
[4]Associate Professor, School of Engineering, University of Warwick, Coventry CV47AL, UK. Email: xueyu.geng@warwick.ac.uk
[5]Associate Professor, Institute of Geotechnical Engineering, College of Civil Engineering, Zhejiang University of Technology, Hangzhou 310000, P.R. China. Email: lishi@zjut.edu.cn
[6]Associate Professor, Institute of Geotechnical Engineering, College of Civil Engineering, Zhejiang University of Technology, Hangzhou 310000, P.R. China. Email: panxd@126.com

Introduction

Currently, land reclamation is an efficient way to address land shortages in coastal areas worldwide. In practice, slurry dredged from the sea bed near the reclamation site is usually used as fill material. However, the slurry has some properties that are extremely unfavorable for further construction, including high water content, low bearing capacity, and high compressibility (Zeng et al., 2016; Lei et al., 2017; Deng et al., 2019, Fang et al., 2019), all of which need to be improved.

Vacuum preloading combined with prefabricated vertical drains (PVDs) is usually used to improve soft soils (Kjellman, 1952; Chu et al., 2000; Tang and Shang, 2000; Saowapakpiboon et al., 2011; Chai et al., 2010; Zhou et al., 2017; Ni et al., 2019; Tian et al., 2019; Wang et al., 2019). That method uses pumps to generate vacuum pressure that causes the hydraulic gradient in the soil to accelerate water drainage (Geng et al., 2012; Indraratna et al., 2004). Compared with other methods, the vacuum preloading method has several important advantages. The increase in effective stress in the soil mass is caused by a decrease in pore water pressure, while total stress remains constant (Liu et al., 2017). Therefore, that method can prevent soil shear failure (Liu et al., 2017), guaranteeing the safety of the treatment process. The vacuum preloading method is also considered to be economical and environmentally friendly (Chai et al., 2010) because it needs no additional materials.

However, recent studies (Liu et al., 2017; Bao et al., 2014; Deng et al., 2018, Zhan et al., 2015, Fu et al., 2017) have reported that poor treatment quality was observed when dredged slurry was treated by the vacuum preloading method. In those cases, when the water discharge rate approached zero, the ground soil still showed low bearing capacity generally. In other words, the soil consolidation stopped, and the average consolidation degree was still much lower than expected. Also, inhomogeneous consolidation was investigated in the improvement of dredged slurries. After consolidation, an area of dense soil formed near the PVD called the clogging zone or soil column. The soil in this zone had high shear strength, low water content, and only slight settlement after the improvement. In contrast, the soil at the peripheral area was still weak, with high water content, low bearing capacity, and large settlement (Tang et al., 2010; Cheng et al., 2010).

Researchers have done several tests to determine the cause of those phenomena. In those tests, fine particles were found penetrating the PVD's geotextile filter jacket, caked on the upstream side of the filter jacket, or obstructing geotextile filter openings (Bergado et al., 1996; Ghosh et al., 2004; Giroud, 2005). Because of the clogging at the filter and core of the PVDs, the water discharge channels of the drains were blocked (Cheng et al., 2010). This resulted in a loss of vacuum pressure along the drain (Wang et al., 2016) and a reduction in discharge capacity over time (Chai et al., 1999; Miura et al., 2000; Ghosh et al., 2004). Moreover, soil properties in the clogging zone and outside the zone varied in many aspects. The proportion of fine particles in the clogging zone was greater than that outside the zone (Wang et al., 2017; Deng et al., 2018; Fang et al., 2019). Those fine particles filled the pores of the soil, reducing compressibility in the clogging zone. The permeability in the clogging zone was also much reduced, which impeded the water drainage and caused poor improvement quality (Fang et al., 2019). Therefore, the causes of poor improvement quality can be summarized in two aspects: the first is clogging occurring at the drain surface, which is manifested as a reduced discharge capacity of the PVDs, and the second is clogging occurring in the soil near the drains. These two aspects are collectively called the clogging effect. To better understand the consolidation of dredged slurries improved by vacuum pressure, it is crucial to explore the effect of clogging on the consolidation behavior at different radial distances from the PVDs.

In recent years, modified consolidation theories have been proposed to predict the consolidation of soft soils considering the clogging effect. Several studies that used laboratory tests to measure the discharge capacity of PVDs (Chai et al., 1999; Kim et al., 2011) proposed to use a time-dependent exponential decrease in discharge capacity in a consolidation theory to consider the influence of the clogging effect (Deng et al., 2013; Nguyen et al., 2016). However, in those studies, solutions were all obtained under equal strain assumptions, which did not consider the varied settlements of the clogging and the outside-clogging zones. Also, those theories involved only surcharge loading, which could not calculate the consolidation of dredged fills under vacuum preloading. On the other hand, analytical consolidation solutions based on a free strain assumption could partially consider the inhomogeneous strain in the radial direction (Barron, 1948; Yoshikuni et al., 1974; Peng et al., 2018). Basu et al. (2000) examined the clogging effect by setting impervious areas of the drain in a finite difference model. Lin et al. (2009) took the influence of clogging into account by imposing a finite discharge capacity on a 3D numerical consolidation model. Cao et al. (2019) simulated the clogging effects by decreasing the equivalent radius of the drain and assuming a new smear zone with low permeability. However, in their work the decrease in discharge capacity was constant in the consolidation process, which is inconsistent with the fact that drain clogging occurs gradually. Oliveira (2013) proposed an empirical formula of discharge capacity relevant to consolidation time and confining pressure and built a finite element model involved a variable discharge capacity, which could calculate the consolidation at various radii. However, the model could not consider the clogging in the soil, and its numerical model was complex.

For this study, a consolidation model is built based on uneven strain assumptions involving a time-dependent decrease in PVD discharge capacity. Analytical solutions are solved out to calculate the consolidation in the clogging zone and outside it considering the clogging effect. Detailed parametric analyses are conducted to show the influence of clogging on the total consolidation degree and the difference in consolidation between the clogging zone and the normal zone. The results calculated by the proposed solution are compared with those of an existing solution based on equal strain assumptions to determine the effect of the uneven strain assumption in the consolidation calculation. Finally, the proposed solutions are applied to a practical case to show its advantages in the calculation of consolidation with the clogging effect.

Mathematical model and analytical solution

To consider the clogging at the drain surface, it is assumed that the discharge capacity of PVDs exponentially decreases in the form of Eq. (1), according to previous studies (Deng et al., 2013; Nguyen et al., 2016)

$$q_w = q_{w0} \mathrm{e}^{-a_w t} \quad \text{or} \quad k_w = k_{w0} \mathrm{e}^{-a_w t} \tag{1}$$

where q_{w0} is the initial discharge capacity of the vertical drain, q_w is the discharge capacity at any time, a_w is the coefficient that denotes the decrease rate of the discharge capacity, k_{w0} is the initial permeable coefficient of the vertical drain, k_w is the permeable coefficient of the vertical drain at any time, e is the natural logarithm, and t is the consolidation time. Other assumptions include the following: (a) the solid particles and the pore fluid are incompressible, (b) the soil is fully saturated at all times, (c) Darcy's flow law is valid, and (d) all deformation occurs in the vertical direction.

Although the clogging effect is supposed to occur in the slurries improved by vacuum preloading, in the present model, to expand the application range of the proposed solution, surcharge loading is also considered. In cases with only vacuum pressure applied, the surcharge loading equals 0. In the model, the effective zone of a PVD is divided into a clogging zone and a normal zone.

The clogging zone has some similarities with the smear zone because both of them are near the drains and have lower permeability than the outside. However, they still have very large differences practically and theoretically. Practically, the smear zone forms because of the insertion and removal of PVDs that destroy the structure of the soil near the drain. Because of the disturbance, horizontal permeability in the smear zone is much lower than that in the outside (Sharma and Xiao, 2000). In contrast, the clogging zone forms only in the improvement of slurries due to the migration of fine particles and nonuniform consolidation under vacuum pressure. Fine particles block the pores of the soil in the clogging zone, reducing permeability and compressibility, which further leads to the inhomogeneous consolidation of the soil. To be mentioned, there are controversial views on the migration of fine particles. Chai et al. (2020) and Wang et al. (2020) believed that the migration of fine particles was not evident during the improvement process of dredged slurries, because the grain size distributions at various radii were almost identical after consolidation in their tests. In contrast, Fang et al. (2019) found the distribution of average particle size along radius changed from the initial homogeneous state to a significantly inhomogeneous state after the improvement. The average particle size was smallest in the area adjacent to the drain, so fine particles were supposed to migrate toward the PVD. The latter view is chosen here because the samples that they used in the particle size distribution tests were collected at around 1/2 depth of the soil element, which could represent a more general situation. Theoretically, in the consolidation model that incorporates the smear effect, only the difference of the permeable coefficient is involved, and the difference of compressibility is ignored. However, the difference of compressibility of the clogging zone and the outside have substantial influences on the consolidation behavior, so both of them are considered in the clogging zone, which is different from the way of considering the smear effect.

The axisymmetric unit cell scheme is shown in Fig. 1, where r_w, r_c, and r_e are the radii of the vertical drain, the clogging zone, and the effective zone respectively; r is the distance of the soil at any point to the center of the drain; k_c and k_h are the radial permeable coefficients in the clogging zone and normal zone respectively; k_r is the permeable coefficient at any radius; p is the vacuum pressure; q is the surcharge loading; and k_1 is the coefficient of vacuum loss along the drain, which is defined as the ratio between the vacuum pressure at the bottom and top of the drain. The drain is assumed to penetrate the soil layer entirely, so the length of the drain (l) is equal to the thickness of the soil (H).

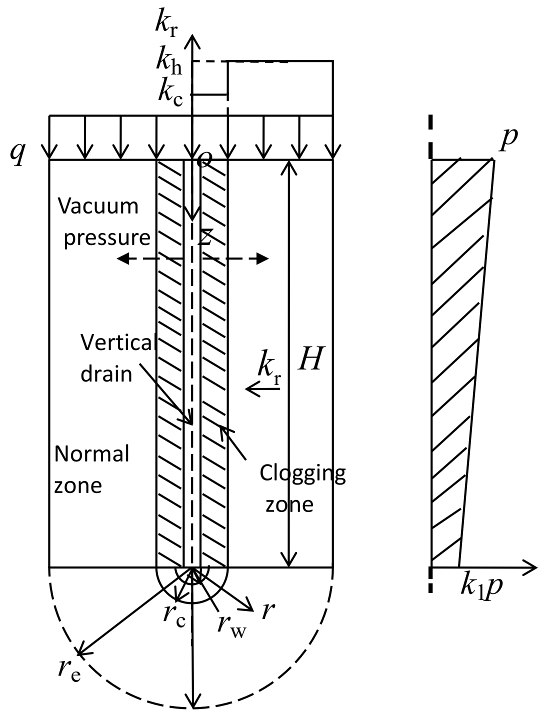

Fig. 1. Analysis scheme of a unit cell with a vertical drain

Because the settlement in the clogging zone was observed to be less than that in the normal zone (Chai et al., 2020), two independent strains are assumed in the model for each zone to consider the clogging in soil, which in this paper is called an uneven strain condition. In the uneven strain condition, an equal strain is assumed in each zone but the strains of the two zones vary. It can be seen as a condition between the equal strain condition and the free strain condition, which can meet the need for calculating settlements at various radii with solutions in the simple form. To build the governing equations separately, the pore water pressures in the two zones are assumed to be two independent governing variables here. According to Hansbo (1981), the governing equations for the clogging zone and the normal zone can be expressed as

$$\begin{cases} -\dfrac{k_c}{\gamma_w}\dfrac{1}{r}\dfrac{\partial}{\partial r}\left(r\dfrac{\partial u_c}{\partial r}\right)=\dfrac{\partial \varepsilon_{vc}}{\partial t} & r_w \le r \le r_c \\ -\dfrac{k_h}{\gamma_w}\dfrac{1}{r}\dfrac{\partial}{\partial r}\left(r\dfrac{\partial u_n}{\partial r}\right)=\dfrac{\partial \varepsilon_{vn}}{\partial t} & r_c \le r \le r_e \end{cases} \tag{2}$$

where γ_w is the unit weight of water, u_c and u_n are the excess pore water pressures in the clogging zone and the normal zone around the drain respectively, and ε_{vc} and ε_{vn} are the consolidation strains in the clogging zone and the normal zone respectively.

Boundary conditions

The outer boundary of the effective zone is assumed to be impermeable. The pore water pressure at the surface between the clogging zone and the normal zone is continuous. In the drain, vacuum pressure penetrates from the upper surface to the bottom with loss, and the pore water pressure at the drain boundary is equal to that at the inner boundary of the clogging zone. Thus, the boundary conditions can be written as (Geng et al., 2012)

$$\begin{aligned} &\text{(a) } r=r_e:\ \frac{\partial u_n}{\partial r}=0 \\ &\text{(b) } r=r_c:\ k_c\frac{\partial u_c}{\partial r}=k_h\frac{\partial u_n}{\partial r}, u_c=u_n \\ &\text{(c) } r=r_w:\ u_w=u_c, \frac{\partial u_c}{\partial r}+\frac{q_w}{2\pi r_w k_c}\frac{\partial^2 u_w}{\partial z^2}=0 \\ &\text{(d) } z=0:\ u_w=p \\ &\text{(e) } z=H:\ \frac{\partial u_w}{\partial z}=\frac{(1-k_1)}{l}p \end{aligned} \tag{3}$$

where u_w is the pore water pressure in the vertical drain.

By integrating Eq. (2) in the r direction with the boundary conditions (a) and (b), the governing equations can be written as

$$\begin{cases} \dfrac{\partial u_n}{\partial r} = \dfrac{1}{2}\left(\dfrac{r_e^2 - r^2}{r}\right)\dfrac{\gamma_w}{k_h}\dfrac{\partial \varepsilon_{vn}}{\partial t},\ r_c < r < r_e \\ \dfrac{\partial u_c}{\partial r} = \dfrac{1}{2}\left(\dfrac{r_e^2 - r_c^2}{r}\right)\dfrac{\gamma_w}{k_c}\dfrac{\partial \varepsilon_{vn}}{\partial t} + \dfrac{1}{2}\left(\dfrac{r_c^2 - r^2}{r}\right)\dfrac{\gamma_w}{k_c}\dfrac{\partial \varepsilon_{vc}}{\partial t},\ r_w < r < r_c \end{cases} \tag{4}$$

Therefore, the differential u_c at the drainage boundary can be obtained by substituting $r = r_w$ into Eq. (4):

$$\left.\frac{\partial u_c}{\partial r}\right|_{r=r_w} = \frac{1}{2}\left(\frac{r_e^2 - r_c^2}{r_w}\right)\frac{\gamma_w}{k_c}\frac{\partial \varepsilon_{vn}}{\partial t} + \frac{1}{2}\left(\frac{r_c^2 - r_w^2}{r_w}\right)\frac{\gamma_w}{k_c}\frac{\partial \varepsilon_{vc}}{\partial t} \tag{5}$$

According to boundary conditions (d) and (e), u_w can be solved to obtain Eq. (6) by integrating Eq. (5) twice for z:

$$\begin{aligned} u_c|_{r=r_w} = u_w = p + p\left(k_1 - 1\right)\frac{z}{l} + \frac{k_c r_w \pi}{q_w}\cdot\left(lz - \frac{1}{2}z^2\right)\left(\frac{r_e^2 - r_c^2}{r_w}\right)\frac{\gamma_w}{k_c}\frac{\partial \varepsilon_{vn}}{\partial t} \\ + \frac{k_c r_w \pi}{q_w}\cdot\left(lz - \frac{1}{2}z^2\right)\left(\frac{r_c^2 - r_w^2}{r_w}\right)\frac{\gamma_w}{k_c}\frac{\partial \varepsilon_{vc}}{\partial t} \end{aligned} \tag{6}$$

Integrating Eq. (4) in the radial direction with the boundary condition shown in Eqs. (6) and (3), u_c and u_n can be expressed as

$$\begin{aligned} u_c = \frac{\gamma_w}{2k_c}\frac{\partial \varepsilon_{vc}}{\partial t}\left(\left(r_c^2 \ln\frac{r}{r_w} - \frac{1}{2}\left(r^2 - r_w^2\right)\right) + \frac{k_c r_w \pi}{q_w}\left(2lz - z^2\right)\left(\frac{r_c^2 - r_w^2}{r_w}\right)\right) \\ + \frac{\gamma_w}{2k_c}\frac{\partial \varepsilon_{vn}}{\partial t}\left(\left(r_e^2 - r_c^2\right)\ln\frac{r}{r_w} + \frac{k_c \pi}{q_w}\left(2lz - z^2\right)\cdot\left(r_e^2 - r_c^2\right)\right) \\ + p\left(1 - \left(1 - k_1\right)z / l\right) \end{aligned} \tag{7}$$

$$u_n=\frac{\gamma_w}{2k_c}\frac{\partial\varepsilon_{vc}}{\partial t}\left(\left(r_c^2\ln\frac{r_c}{r_w}-\frac{1}{2}\left(r_c^2-r_w^2\right)\right)+\frac{2k_cr_w\pi}{q_w}\left(lz-\frac{1}{2}z^2\right)\left(\frac{r_c^2-r_w^2}{r_w}\right)\right)$$
$$+\frac{\gamma_w}{2k_h}\frac{\partial\varepsilon_{vn}}{\partial t}\left(r_e^2\ln\frac{r}{r_c}-\frac{1}{2}\left(r^2-r_c^2\right)+\frac{k_h}{k_c}\left(r_e^2-r_c^2\right)\ln\frac{r_c}{r_w}+\frac{k_hr_w\pi}{q_w}\left(2lz-z^2\right)\cdot\left(\frac{r_e^2-r_c^2}{r_w}\right)\right)$$
$$+p\left(1-\left(1-k_1\right)z/l\right) \quad (8)$$

Because the equal strain assumption is adopted in the clogging zone and the normal zone separately, the mean pore water pressure in each zone is calculated by

$$\begin{cases}\overline{u}_c=\dfrac{1}{\pi\left(r_c^2-r_w^2\right)l}\displaystyle\int_0^l\int_{r_w}^{r_c}2\pi u_crdrdz\\ \overline{u}_n=\dfrac{1}{\pi\left(r_e^2-r_c^2\right)l}\displaystyle\int_0^l\int_{r_c}^{r_e}2\pi u_nrdrdz\end{cases} \quad (9)$$

In this study, the linear compressibility relation is considered, which can be expressed as $\partial\varepsilon_{vc}/\partial t$=-$m_{vc}\partial u_c/\partial t$ and $\partial\varepsilon_{vn}/\partial t$=-$m_{vn}\partial u_n/\partial t$ in the clogging zone and the normal zone respectively, where m_{vc} and m_{vn} are the coefficients of compressibility in the clogging zone and normal zone respectively. Substituting Eqs. (7) and (8) into Eq. (9), the mean pore water pressure can be derived as

$$\begin{cases}\overline{u}_c=\left(\overline{A}_{11}\mathrm{e}^{a_wt}+\overline{A}_{12}\right)\dfrac{\partial\overline{u}_c}{\partial t}+\left(\overline{A}_{21}\mathrm{e}^{a_wt}+\overline{A}_{22}\right)\dfrac{\partial\overline{u}_n}{\partial t}+\dfrac{1}{2}p\left(1+k_1\right),\ r_w<r<r_c\\ \overline{u}_n=\left(\overline{B}_{11}\mathrm{e}^{a_wt}+\overline{B}_{12}\right)\dfrac{\partial\overline{u}_c}{\partial t}+\left(\overline{B}_{21}\mathrm{e}^{a_wt}+\overline{B}_{22}\right)\dfrac{\partial\overline{u}_n}{\partial t}+\dfrac{1}{2}p\left(1+k_1\right),\ r_c<r<r_e\end{cases} \quad (10)$$

where $\overline{A}_{11}$, $\overline{A}_{12}$, $\overline{A}_{21}$, $\overline{A}_{22}$, $\overline{B}_{11}$, $\overline{B}_{12}$, $\overline{B}_{21}$, and $\overline{B}_{22}$ are time-independent coefficients (detailed in Appendix I).

Initially, the excess pore water pressure is assumed to be equal to the surcharge loading. That is, $u_{c0}=q$ and $u_{n0}=q$, where u_{c0} and u_{n0} are the initial excess pore water pressure in the clogging and normal zones respectively. Then, by applying the initial condition, the mean pore water pressure in the clogging and normal zones can be solved out as

$$\begin{cases} \overline{u}_c = \left(q - \dfrac{1}{2}p\left(1+k_1\right)\right)\left(\left(\dfrac{P_1\mathrm{e}^{J_1} - P_2\mathrm{e}^{J_2}}{P_1 - P_2}\right) - \left(\dfrac{P_1P_2\left(\mathrm{e}^{J_1} - \mathrm{e}^{J_2}\right)}{P_1 - P_2}\right)\right) + \dfrac{1}{2}p\left(1+k_1\right) \\ \overline{u}_n = \left(q - \dfrac{1}{2}p\left(1+k_1\right)\right)\left(\left(\dfrac{P_1\mathrm{e}^{J_2} - P_2\mathrm{e}^{J_1}}{P_1 - P_2}\right) + \left(\dfrac{\mathrm{e}^{J_1} - \mathrm{e}^{J_2}}{P_1 - P_2}\right)\right) + \dfrac{1}{2}p\left(1+k_1\right) \end{cases} \tag{11}$$

where J_1 and J_2 are the eigenvalues of Jordan standard form, and P_1 and P_2 are the eigenvalues of an invertible matrix to obtain the Jordan standard form. The expressions of J_1, J_2, P_1, and P_2 are shown in Appendix II.

On that basis, the degree of consolidation in the clogging zone (U_c) and the normal zone (U_n) in the form of pore water pressure can be expressed as

$$\begin{cases} U_c = \dfrac{q - \overline{u}_c}{q - p} \\ U_n = \dfrac{q - \overline{u}_n}{q - p} \end{cases} \tag{12}$$

The degree of consolidation in the whole effective zone (U) can be written as

$$U = \frac{\overline{u}_c\left(r_c^2 - r_w^2\right) + \overline{u}_n\left(r_e^2 - r_c^2\right)}{r_e^2 - r_w^2} \tag{13}$$

Verification

To verify the proposed solution, the well resistance, the clogging effect, and the uneven strain are ignored to reduce the proposed solution into a conventional solution (Hansbo, 1981). Parameters from Hansbo's (1981) cases are used here for convenience, where $q_w = +\infty$, $r_e = 1$ m, $r_w = 0.25$ m, $H = 20$ m, and $c_h = 1.64 \times 10^{-3}$ m^2/d. c_h is the consolidation coefficient calculated by $c_h = k_h/(m_v\gamma_w)$, and it is substituted as the total value of $k_h/(m_v\gamma_w)$ in the calculation of the proposed solution. The well resistance is ignored by defining q_w in the proposed solution as $+\infty$. Then, r_c is valued at 0.25001 in the verification to make the area of the clogging zone close to 0. Therefore, to eliminate the influence of an uneven strain assumption, the solution can be seen as that for only one average strain. The consolidation coefficient in the clogging zone is equal to that in the normal zone to reduce the effect of clogging in the soil. It can be seen from Fig. 2 that results calculated by the proposed solution fit well with that of Hansbo's (1981) solution, which proves the reliability of the proposed solution.

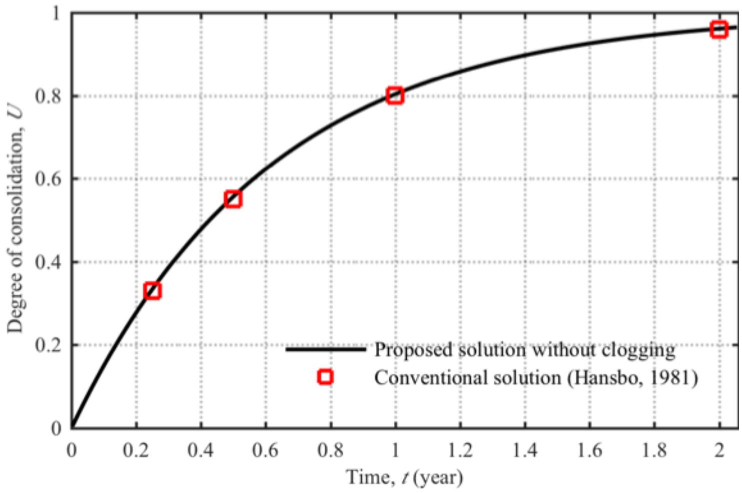

Fig. 2. Comparison between the proposed solution and that of Hansbo (1981)

Parametric analysis

In this section, the effects of clogging on the total consolidation degree, the differences in consolidation between the clogging zone and normal zone, and the influences of the uneven strain assumption are observed. Because the clogging effect included the decay of discharge capacity and the decrease in compressibility and permeability in the clogging zone, parametric analyses are conducted around the parameters related to these two aspects.

According to the data from laboratory tests (Fang et al., 2019), the permeability of the clogging zone could be 1% of that in the normal zone, which is much lower than that in the smear zone and that caused by nonuniform consolidation (Zhou et al., 2017). Therefore, to consider the clogging in the soil, the permeability ratio (k_c/k_h) is assumed to be 1/50 in the following cases. Other parameters are the same as those in Deng et al. (2013), where r_e = 0.525 m, r_c = 0.175 m, r_w = 0.035 m, $k_h = 2 \times 10^{-8}$

m/s, $k_w = 1 \times 10^{-3}$ m/s, $H = 20$ m, $m_{vc} = m_{vn} = 0.2$ MPa^{-1}, $\gamma_w = 10$ kPa/m, and $k_1 = 1$.

The effect of the time-dependent decay coefficient of discharge capacity (a_w)

As stated in Deng et al. (2013), the value of a_w and α can describe the rate of discharge capacity variation where $\alpha = 4a_w r_e^2/c_h$. Fig. 3 shows the variation of discharge capacity over time under various α, where the abscissa is the normalized time factor (T_h) calculated by $T_h = c_h t/d_e^2$. The larger α is, the more rapidly the discharge capacity decreases. An α close to 0 represents a situation where the discharge capacity keeps constant with the elapsed time. Therefore, to cover most situations α is selected to be 1.1×10^{-6}, 0.5, and 1. The corresponding values of a_w are 10^{-11}/s, 4.54×10^{-6}/s, and 9.07×10^{-6}/s, among which $a_w = 10^{-11}$/s represents a case with no clogging at the drain.

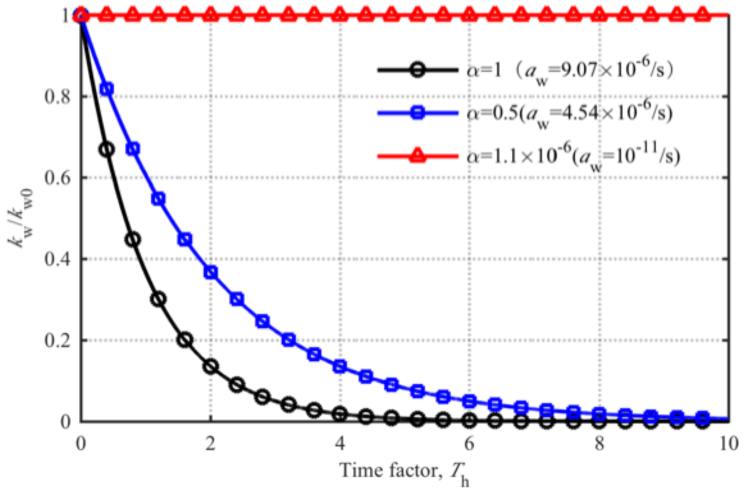

Fig. 3. Variations in discharge capacity with various α

Fig. 4(a) shows the degree of consolidation in the whole area as calculated by the uneven strain solution proposed in this paper and as calculated by the equal strain solutions (Nguyen et al., 2016) with various a_w. When a_w approaches 0, the consolidation can complete in a limited time as usual. In contrast, when $a_w = 4.54 \times 10^{-6}$/s and 9.07×10^{-6}/s, the degree of consolidation could not reach 100%. In these cases, the discharge capacity decreases to 0 quickly, as shown in Fig. 3, because the severe clogging of PVDs hinders the water flow and stops the consolidation. Moreover, it can be found that the final degree of consolidation decreases with the increase in a_w, as reported by Deng et al. (2013). The final degree of consolidation calculated by the proposed solution is 12% larger than that calculated by the equal strain solution when $a_w = 4.54 \times 10^{-6}$/s, which is the largest among the three cases. When $a_w = 9.07 \times 10^{-6}$/s, the difference between the solutions based on the equal strain assumption and the uneven strain assumption is 10%. For the case without clogging at the drain, the uneven strain assumption has almost no influence on the final consolidation degree. The cause of this difference is provided below based on the comparison of consolidation in the clogging zone and that in the normal zone.

Fig. 4(b) shows the degrees of consolidation in the clogging and normal zones with different decay coefficients. It can be found that the consolidation in the normal zone proceeds steadily. In contrast, the increase in the consolidation degree in the clogging zone is sharp at the beginning but gentle at the end. Moreover, the consolidation degree in the clogging zone is always larger than that in the normal zone from the beginning to the end. Therefore, the decay of discharge capacity could be a factor that causes uneven consolidation in slurries improved by vacuum pressure.

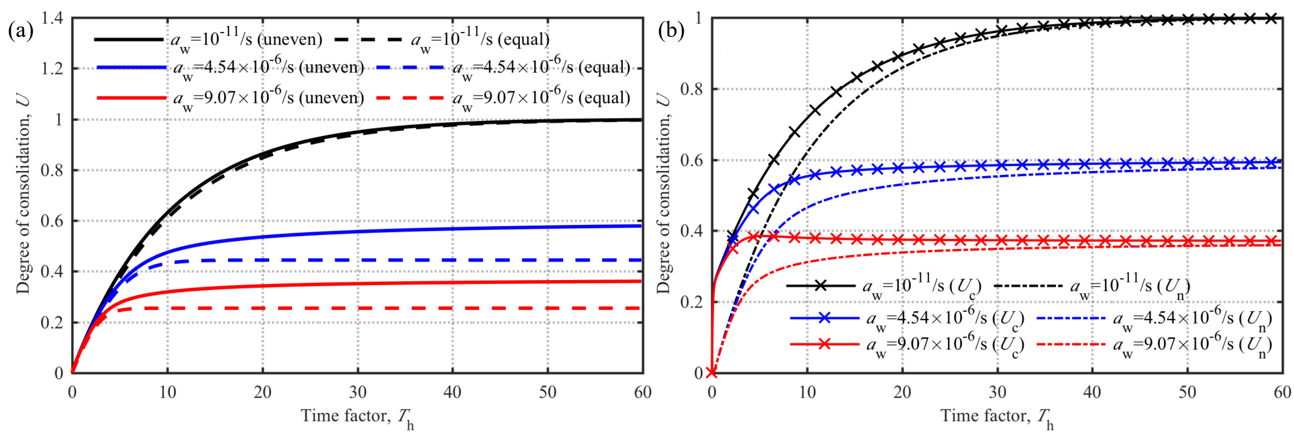

Fig. 4. Effect of the decay speed of the discharge capacity on the consolidation degree: (a) the total effective zone; (b) the clogging and normal zones

Because the clogging zone has larger consolidation degree than the normal zone has, the consolidation degree calculated by Nguyen at al. (2016), which represents the average in the entire effective zone, is less than that in the clogging zone. Fig. 3 shows that the discharge capacity decreases to 0 at approximately T_h = 10 when $a_w = 4.54 \times 10^{-6}$/s and at T_h = 5 when $a_w = 9.07 \times 10^{-6}$/s. At that time, the increase in consolidation degree in the clogging zone calculated by the proposed solution and that in the whole zone calculated under the equal strain assumption almost stops. After that, although the water discharge speed is quite low, the consolidation of the normal zone could still proceed until the hydraulic gradient between the clogging zone and the normal zone disappears. The proposed solution can consider the consolidation in this stage, but the equal strain assumption cannot. Thus, the final degree of consolidation in the entire effective zone calculated by the proposed method is greater. Fig. 4(b) shows that in the cases with $a_w = 4.54 \times 10^{-6}$/s and 9.07×10^{-6}/s, the difference between the clogging zone and the normal zone is more evident than $a_w = 10^{-11}$/s. Therefore, the difference between the consolidation degree in the clogging zone and the average in the whole zone that can be regarded as that in the equal strain solution, is larger when q_w approached 0. Because the final consolidation degree in the whole zone equals the degree of consolidation in the clogging zone, the difference between the two solutions is greater when a_{w} is larger generally.

The effect of the initial discharge capacity (k_{w0})

In this section, the effect of the initial discharge capacity on the consolidation is described by changing the value of k_{w0} while keeping other parameters unchanged. In Fig. 5(a), the consolidation is calculated with no clogging at the drain considered, whereas in Fig. 5(b) the clogging at the drain is considered by setting $a_w = 4.54 \times 10^{-6}$/s. Comparing the results for the same k_{w0} in Figs. 5(a) and 5(b) shows that the difference between the consolidation degree with and without considering clogging increases with the decrease in k_{w0}. That is, the impact of clogging increased with the decrease in initial discharge capacity. Moreover, it can be seen that the difference between the equal strain solution and the uneven strain solution is more obvious for cases with larger k_{w0}/k_h when clogging at the drain is considered. The maximum difference of consolidation degree between the two solutions is 3.8% for cases with $k_{w0}/k_h = 5 \times 10^3$. Then, it can be derived that either the equal strain assumption or the uneven strain assumption can be used when k_{w0}/k_h is less than 5×10^3.

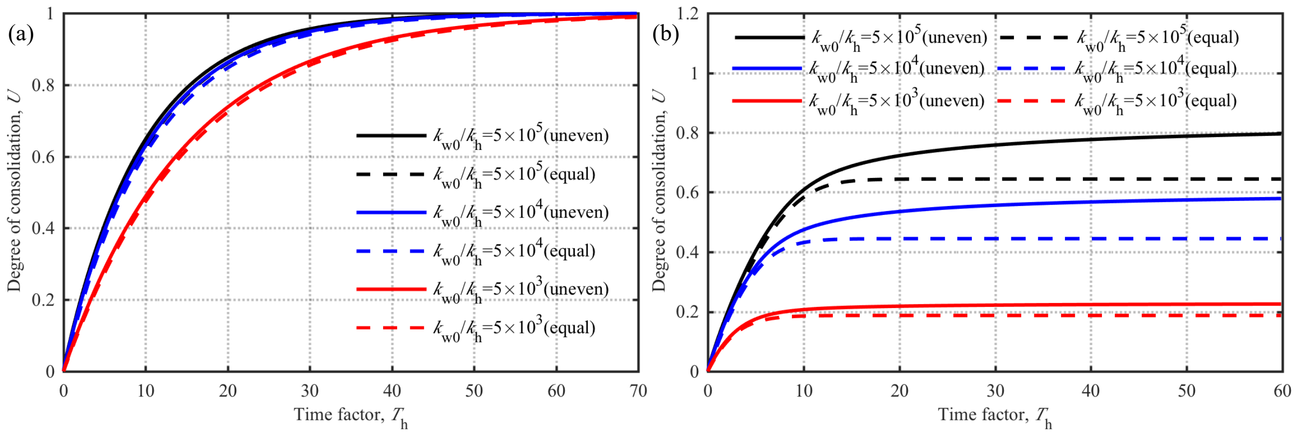

Fig. 5. Effect of initial discharge capacity on consolidation degree for total effective zone: (a) without clogging at the drain (a_w =10^{-11}/s); (b) with clogging at the drain (a_w = 4.54×10^{-6}/s)

Fig. 6 shows the degrees of consolidation in the clogging zone and the normal zone with various k_{w0}/k_h when discharge capacity decay is considered. With the decrease in initial discharge capacity, the difference between the two areas decreased. Therefore, the larger difference between the solutions based on the uneven strain assumption and the equal strain assumption for greater k_{w0}/k_h can be explained in the same way as stated in the last section.

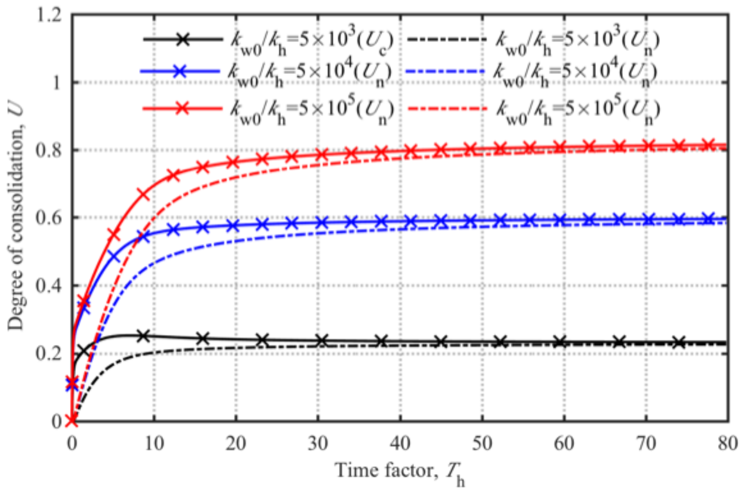

Fig. 6. Effect of initial discharge capacity on consolidation degree for the clogging and normal zones with $a_w = 4.54 \times 10^{-6}$/s

The effect of the permeability ratio (k_c/k_h)

Fig. 7 shows the consolidation degrees with various permeability ratios. When regarding the discharge capacity as a constant, the value of the permeability ratio affects only the consolidation speed, as shown in Fig. 7(a). The speed of consolidation decreases as k_c/k_h decreases. Fig. 7(b) shows that when the decay of discharge capacity is considered, the final consolidation degree decreases with the decrease in the permeability ratio. Compared with the consolidation shown in Fig. 7(a), the lower permeability ratio influences the consolidation more markedly. Because cases with k_c/k_h = 1/5 can represent the consolidation of normal soft soil, the results indicate that clogging in the soil is an important component of the clogging effect on the consolidation. It can be seen in Fig. 7(b) that the ratio of k_c/k_h affects the difference between the two solutions when the discharge capacity decays. The deviation for k_c/k_h = 1/5 is 4%, whereas that for k_c/k_h = 1/50 and 1/100 is 12%. The influence of the uneven assumption is more substantial when clogging occurs in the soil. Thus, when k_c/k_h is greater than 1/5, the influence of the uneven strain assumption could be ignored in the calculation of consolidation with discharge capacity decay.

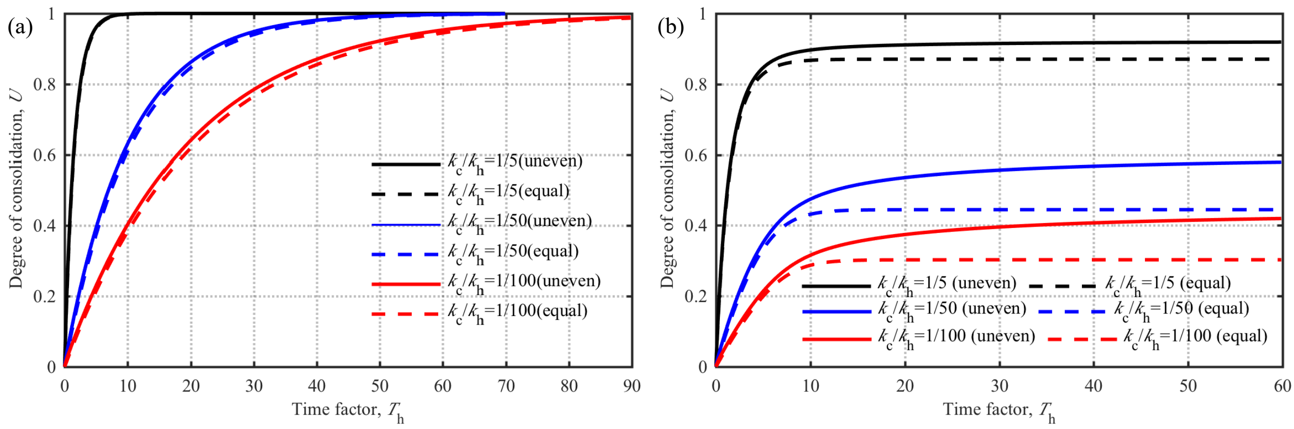

Fig. 7. Effect of permeability ratio on consolidation degree for total effective zone: (a) without clogging at the drain ($a_w = 10^{-11}$/s); (b) with clogging at the drain ($a_w = 4.54 \times 10^{-6}$/s)

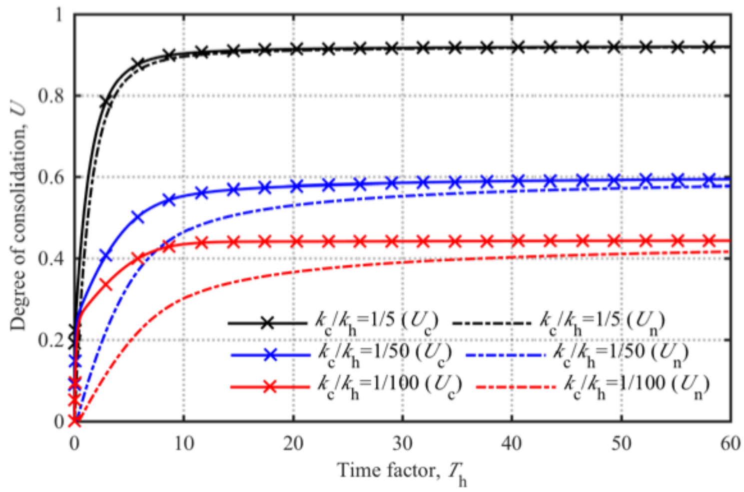

Fig. 8. Effect of permeability ratio on consolidation degree for clogging and normal zones with $a_w =$ 4.54×10^{-6}/s

Fig. 8 shows the consolidation degree in the clogging and normal zones with discharge capacity decay. It can be concluded that the degree of consolidation in the normal zone approaches that in the clogging zone slowly after the rapid growth stage. Moreover, the difference of consolidation degree between the clogging zone and the normal zone increases with the decrease in permeability ratio. This is because the vacuum pressure penetrates the normal zone rapidly when the permeability in the clogging zone is high. Therefore, in laboratory and field tests, in the soil with clogging, the consolidation is usually observed to be nonuniform, whereas there is no evident difference between the two zones in the cases without clogging.

The effect of clogging radius (r_c)

In the field and laboratory tests, the radius of the clogging zone is found to be approximately 1–7 times the equivalent radius of the vertical drain, which is detailed in Table 1. Thus, $r_c = 2.5r_w$, $5r_w$, and $7.5r_w$ are applied in the present work to study the effect of the clogging radius. Other parameters are the same as before.

Table 1. Laboratory investigation of clogging radius

Source	r_w (m)	r_c (m)	r_c/r_w
Cheng et al.(2010)	0.033	0.075-0.125	2.27-3.78
Shen (2015)	0.033	0.07	2.12
Fang et al. (2019)	0.008	0.054	6.75

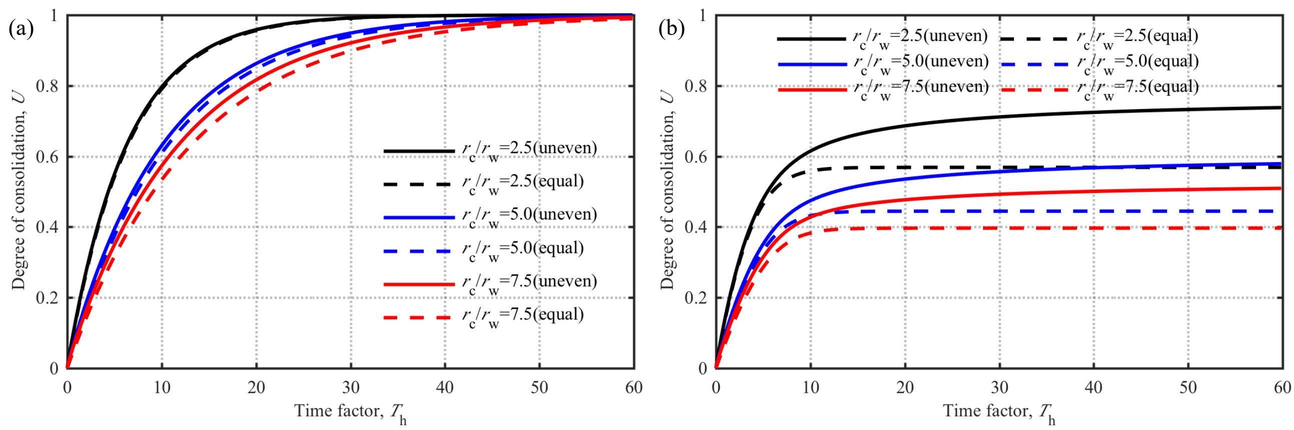

Fig. 9. Effect of clogging radius on consolidation degree for total effective zone: (a) without clogging at the drain ($a_w = 10^{-11}$/s); (b) with clogging at the drain ($a_w = 4.54 \times 10^{-6}$/s)

Fig. 9 shows the consolidation behavior of soil in the entire zone under various values of r_c/r_w with and without a decay of the discharge capacity. Comparing the results in Figs. 9(a) and 9(b) shows that when the discharge capacity decay is considered, the increase in the clogging radius lead to a decrease in the final degree of consolidation. This is reasonable because the increase in the low-permeability area reduces the whole permeability in the soil. Because of that, the amount of water drainage decreases at the stage when the discharge capacity of the drain is still high. This stage is supposed to be the most efficient stage for water drainage. Therefore, the influence of clogging is more obvious in cases with larger clogging radii. Fig. 9(b) shows that all the differences between the equal strain solution and the uneven strain solution in these cases are over 10% when the decay of discharge capacity is considered, so the influence of uneven strain cannot be ignored regardless of the radius of the clogging zone. Besides, the difference between the two solutions increases slightly with a decrease in the clogging radius. This can be explained by the fact that the average excess pore water pressure in the equal strain solution is closer to that of the clogging zone in the uneven strain solution when the larger radius of the clogging zone is considered. Therefore, the consolidation degree under the equal strain assumption is closer to that in the results of the clogging zone when q_w approaches 0. Because the final consolidation degree calculated by the proposed solution is decided by that in the clogging zone, the decrease in the difference between the two solutions shown in Fig. 9(b) is reasonable. Fig. 10 shows that the radius of the clogging zone has little influence on the difference between the consolidation degree in the clogging zone and the normal zone.

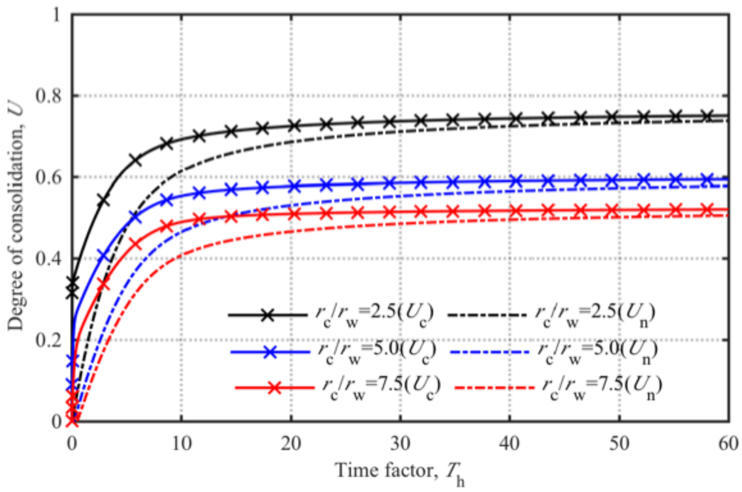

Fig. 10. Effect of clogging radius on consolidation degree for clogging and normal zones with a_w = 4.54×10^{-6}/s

The effect of the compressive coefficient ratio (m_{vc}/m_{vn})

Fang et al. (2019) showed that the compressive coefficient in the normal zone was approximately 1–4 times that in the clogging zone. Thus, to study the effect of compressibility variation m_{vc}/m_{vn} = 1, 1/2, and 1/3 are used. Because the equal strain consolidation cannot consider various m_v in different zones, the value of m_{vc}/m_{vn} is set as 1 in the calculation.

Fig. 11 compares the consolidation degree under different values of m_{vc}/m_{vn} with and without considering discharge capacity decay. Fig. 11(a) shows that the results in cases without decay of discharge capacity are almost the same regardless of the value of the compressive coefficient ratio. In contrast, it can be seen in Fig. 11(b) that cases with smaller m_{vc}/m_{vn} have larger degrees of consolidation when discharge capacity decay is considered, but the difference is small. Therefore, the value of compressibility has little influence on the decrease in consolidation degree caused by the clogging effect. The difference in consolidation degree between the results calculated by the two solutions is almost the same for cases with various compressive coefficient ratios.

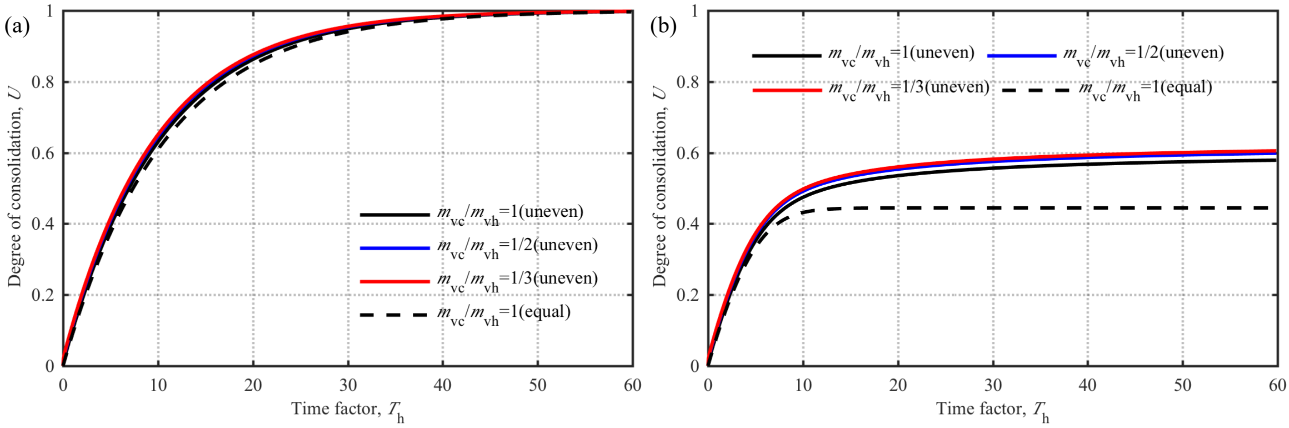

Fig. 11. Effect of compressibility ratio on consolidation degree for total effective zone: (a) without clogging at the drain ($a_w = 10^{-11}$/s); (b) with clogging at the drain ($a_w = 4.54 \times 10^{-6}$/s)

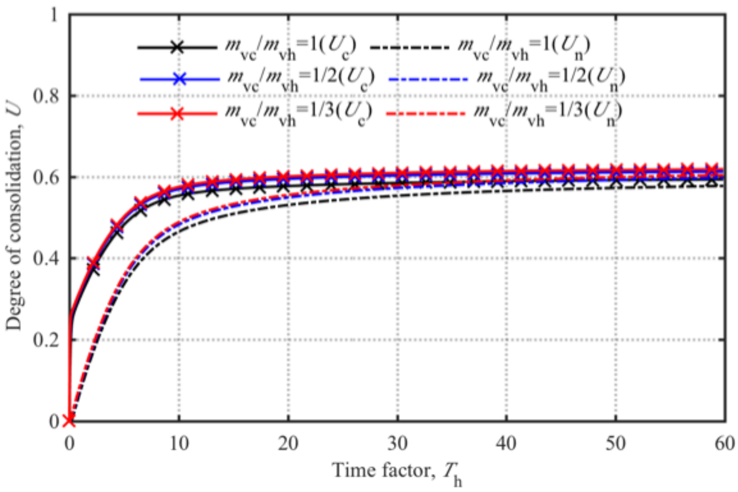

Fig. 12. Effect of compressibility ratio on consolidation degree for clogging and normal zones with $a_w = 4.54 \times 10^{-6}$/s

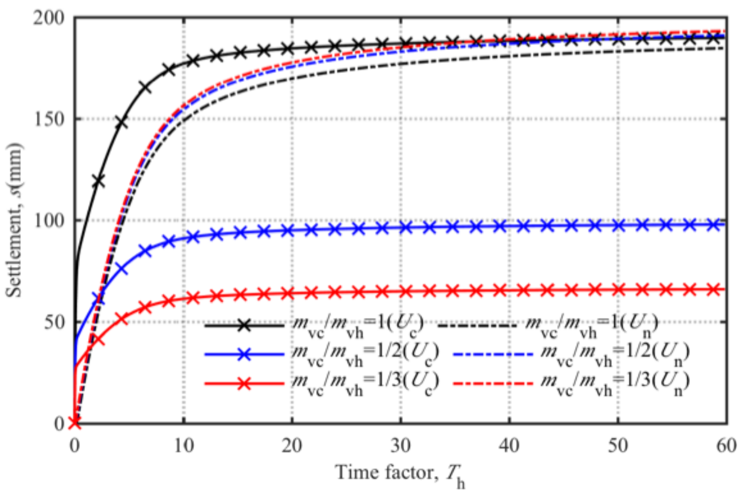

Fig. 13. Effect of compressibility ratio on settlements for clogging and normal zones with a_w = 4.54

$\times\ 10^{-6}$/s

Fig. 12 shows the effect of m_{vc}/m_{vn} on the consolidation degree in two zones when clogging at the drain and the soil are both considered. It can be seen that the differences between the two zones are almost the same with various m_{vc}/m_{vn}. Settlements in the clogging zone and the normal zone are shown in Fig. 13 with various m_{vc}/m_{vn} considered. When the compressibility is the same in the two zones, the settlement of the clogging zone is greater than that of the normal zone because the degree of consolidation in the clogging zone is greater. In contrast, the settlement of the clogging zone is first greater and then much smaller than that of the normal zone when the compressibility of the clogging zone is smaller than that of the normal zone. As stated before, the degree of consolidation in the normal zone is much smaller than that in the clogging zone at first, and then approaches it. The compressibility is low in the clogging zone, but the effective stress increase is so large at first that the settlement in it is larger than that in the normal zone. In the end, the consolidation degrees in the two zones are almost the same in cases with different compressive coefficient ratios. The comparison results here are consistent with the observation that settlement in the clogging zone is always smaller than that in the normal zone in many field tests, as stated in the introduction. Furthermore, the difference between settlements of the two zones increases with the decrease in the compressive coefficient ratio, so the influence of the uneven strain assumption slightly increases.

Case study

Laboratory tests were carried out by Wang et al. (2018) to investigate the variations in settlement, pore water pressure, and vacuum pressure during the consolidation process of dredged slurries improved by vacuum pressure. The soil in those tests was obtained from the Oufei reclamation site in Wenzhou, China. The height of the soil in the model test was designed to be 1,400 mm, and the PVDs were installed in a square pattern at a spacing of 500 mm. Vacuum pressure was applied instantaneously and maintained at 80 kPa for 672 hours. Settlement plates were placed on the surface and in the soil. Pore water pressure was also measured by transducers at different depths.

As found by Hong et al. (2010) and Cao et al. (2014), compressibility and permeability of dredged fills are related to the void ratio, which can be expressed as

$$e = \begin{cases} -0.06 e_L^{-4.91} e_0^{2.77e_L^2 - 10.49e_L + 13.3} \sigma' + e_0 & \sigma' < \sigma'_s \\ C_c^* \left[3.0 - 1.87 \lg \sigma' + 0.179 \left(\lg \sigma' \right)^2 \right] + e_{100}^* & \sigma' \geq \sigma'_s \end{cases} \tag{14}$$

where e and e_0 are the void ratios of the soil at any time and at the initial time respectively, e_L is the void ratio of soil at the liquid limit, σ' is the effective stress, σ'_s is the remolded yield stress, C_c^* is the inherent compression parameter, and e_{100}^* is the void ratio of remolded soil at an effective stress of 100 kPa, which can be expressed as

$$\begin{cases} \sigma'_s = 5.66 / \left(e_0 / e_L \right)^2 \\ e_{100}^* = 0.109 + 0.607 e_L - 0.089 e_L^2 + 0.016 e_L^3 \\ C_c^* = 0.256 e_L - 0.04 \end{cases} \tag{15}$$

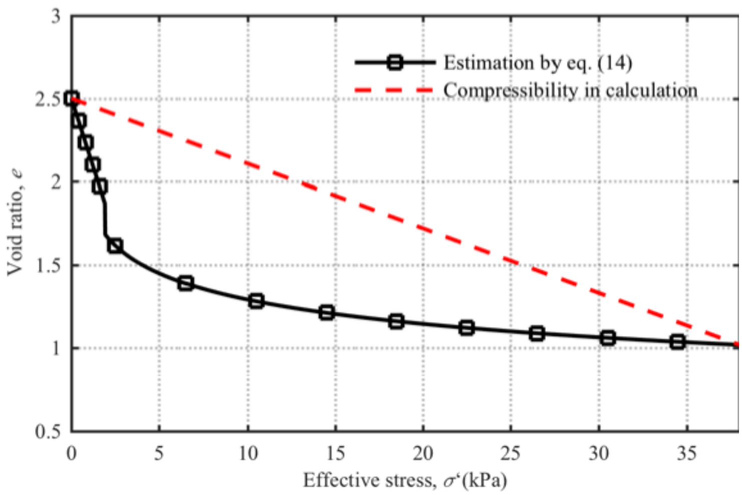

Fig. 14. Evaluation of soil compressibility

Because the samples were fully saturated, we calculated the e_L to be 1.46. Because the soil was ultrasoft, with a water content over the liquid limit and with essentially no shear strength (Wang et al., 2018), the effective stress could be considered as 0 initially, which could also be obtained by substituting e_0 into Eq. (14). Because the final reduction of the pore water pressure was measured to be 38 kPa at the boundary of the effective zone, the compressibility curve of this sample could be drawn according to Eq. (15), and the coefficient of compressibility is assumed to be –11 MPa^{-1}, as Fig. 14 shows. The difference between the water content at 10 cm and 20 cm away from the PVD was reported, so the effective zone is divided into a clogging zone and a normal zone in the calculation on that basis. For the convenience of verification, radius of the clogging zone is assumed to be $5r_w$, dividing the two observation points into two zones. This assumption also matches the ratio of r_c/r_w mentioned before. To consider clogging occurring in the soil, the ratio between the permeable coefficient in the clogging zone and that in the normal zone is assumed to be 1/50 considering the results from Fang et al. (2019), and the compressibility ratio is assumed to be 1/2. To consider the clogging at the drain, vacuum loss coefficient (k_1) is determined to be 0.75 according to the measured vacuum pressure along the drain (Wang et al., 2018). In the measurement by Deng et al. (2016), a_w was calculated to be 0.015/h, which is also used in the calculation. Four cases are calculated to compare different solutions; the parameters used in these cases are summarized in Table 2. Among them, case A involves the full clogging effect, whereas cases B and C consider only the clogging in the soil and at the drain respectively. Case D is calculated using the solution based on the equal strain assumption (Nguyen et al., 2016). Fig. 15 shows the comparison of excess pore water pressures calculated in different cases with the measured value. It can be seen that the proposed solution considering the clogging effect in both the drain and the soil fit well with the test results. The deviation at the early stage is caused by an underestimation of compressibility. The solution where the decay of the discharge capacity or the clogging of the soil is ignored greatly overestimates the dissipation of pore water pressure. Therefore, the consideration of clogging both at the drain and in the soil is necessary when calculating the consolidation of dredged slurry improved by vacuum pressure. The solution based on the equal strain assumption also fits well here, but the consolidation calculated by it ends earlier than the measurements, which may cause errors later. Thus, the uneven strain assumption is necessary for predicting consolidation with the clogging effect.

Table 2. Parameter values used in the simulation

Parameter	Case A	Case B	Case C	Case D
e_0	2.5			
k_w (cm·s^{-1})	5×10^{-3}			
L(m)	1.4			
r_w (m)	0.026			
k_h (cm·s^{-1})	5.26×10^{-5}			
m_{vn} (MPa^{-1})	-11			
d_e (m)	0.564			
r_c/ r_w	5			
p (kPa)	-80			
a_w (s^{-1})	0.015	10^{-11}	0.015	0.015
k_1	0.75	1	0.75	1
k_c/ k_h	1/50	1/50	1/5	1/50
m_c/ m_n	1/2	1/2	1	1

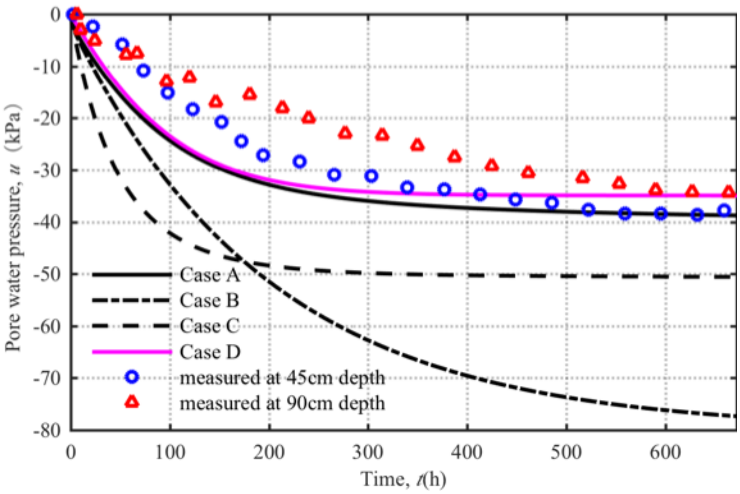

Fig. 15. Comparison of the measured and calculated excess pore water pressure

Conclusion

This study derives analytical solutions for slurries with clogging by considering the time-dependent discharge capacity of the vertical drain and the small permeability ratio in the soil under the uneven strain assumption. When the proposed solution is applied to a case study, a reasonable prediction compared with the test data could be observed. After that, a series of parametric analyses are conducted to study the influences of the clogging effect, the differences in consolidation between the clogging zone and the normal zone, and the effect of the uneven strain assumption. The main results are summarized as follows:

(1) To improve the effectiveness of the consolidation calculation of dredged slurries treated by vacuum pressure, the clogging effect should be considered. This effect slows the development of consolidation and reduces the final consolidation degree. Moreover, the effect of clogging on consolidation is more substantial in cases with a faster decay of discharge capacity, a smaller initial discharge capacity of the drain, a lower permeability in the clogging zone, or a larger clogging radius.

(2) In contrast to a solution based on an equal strain assumption, the proposed solution based on an uneven strain assumption can calculate the consolidation in the clogging zone and the normal zone

separately with different compressibility in the two zones. For example, assuming the compressive coefficient ratio (m_{vc}/m_{vn}) is less than 1 in soil with clogging, the settlement in the clogging zone can be calculated out by the proposed solution to be less than that in the normal zone, which cannot be determined by the equal strain solution. The consolidation degree calculated by the proposed solution is higher than that calculated by the equal strain solution when the clogging effect is considered. However, the influence of uneven strain on the consolidation degree can be ignored when k_{w0}/k_h is less than 5×10^3 or when k_c/k_h is less than 1/5.

(3) The difference in consolidation between the clogging zone and the normal zone is more evident when a smaller k_{w0}/k_h or k_c/k_h is applied. Compared with the cases without clogging, the difference between the clogging zone and the normal zone in the slurries with clogging can last for a long time, far beyond the observation time. The decay of discharge capacity combined with low permeability and low compressibility in the clogging zone is the cause of the inhomogeneous consolidation observed in engineering practice.

Appendix I

The coefficients in Eq. (10) can be expressed as

$$
\begin{aligned}
&\text{(a) } \bar{A}_{11} = -\frac{\gamma_w m_{vc} L^2 \pi \left(r_c^2 - r_w^2\right)}{3q_{w0}},\\
&\text{(b) } \bar{A}_{12} = -\frac{\gamma_w m_{vc}}{2k_c} \frac{\left(-3r_c^4 + 4r_c^2 r_w^2 - r_w^4 + 4r_c^4 \ln\left(r_c / r_w\right)\right)}{4\left(r_c^2 - r_w^2\right)},\\
&\text{(c) } \bar{A}_{21} = -\frac{\gamma_w m_{vn} L^2 \pi \left(r_c^2 - r_e^2\right)}{3q_{w0}},\\
&\text{(d) } \bar{A}_{22} = -\frac{\gamma_w m_{vn}}{2k_c} \frac{\left(\left(r_c^2 - r_w^2\right)\left(r_c^2 - r_e^2\right) + 2r_c^2\left(r_e^2 - r_c^2\right)\ln\left(r_c / r_w\right)\right)}{2\left(r_c^2 - r_w^2\right)},\\
&\text{(e) } \bar{B}_{11} = \frac{m_{vc} \gamma_w L^2 \pi \left(r_c^2 - r_w^2\right)}{3q_{w0}},\\
&\text{(f) } \bar{B}_{12} = -\frac{m_{vc} \gamma_w}{2k_c} \frac{\left(2r_c^2 \ln\left(r_c / r_w\right) - \left(r_c^2 - r_w^2\right)\right)}{2},\\
&\text{(g) } \bar{B}_{21} = -\frac{m_{vn} \gamma_w L^2 \pi \left(r_c^2 - r_e^2\right)}{3q_{w0}},\\
&\text{(h) } \bar{B}_{22} = -\frac{m_{vn} \gamma_w}{2k_h} \frac{4k_c r_e^4 \ln\left(r_e / r_c\right) - k_c\left(r_c^2 - r_e^2\right)\left(r_c^2 - 3r_e^2\right) + 4k_h\left(r_c^2 - r_e^2\right)^2 \ln\left(r_c / r_w\right)}{4k_c\left(r_e^2 - r_c^2\right)}
\end{aligned}
\tag{16}
$$

Appendix II

The expressions of J_1, J_2, P_1, and P_2 can be written as

$$
\begin{aligned}
&\text{(a) } P_1 = \frac{D_{11}}{2D_{21}} + \frac{D_{22}}{2D_{21}} - \frac{\left(D_{11}^2 - 2D_{11}D_{22} + D_{22}^2 + 4D_{12}D_{21}\right)^{(1/2)}}{2D_{21}} - \frac{D_{22}}{D_{21}},\\
&\text{(b) } P_2 = \frac{D_{11}}{2D_{21}} + \frac{D_{22}}{2D_{21}} + \frac{\left(D_{11}^2 - 2D_{11}D_{22} + D_{22}^2 + 4D_{12}D_{21}\right)^{(1/2)}}{2D_{21}} - \frac{D_{22}}{D_{21}},\\
&\text{(c) } J_1 = \frac{1}{2}\left(D_{11} + D_{22} - \left(D_{11}^2 - 2D_{11}D_{22} + D_{22}^2 + 4D_{12}D_{21}\right)^{(1/2)}\right),\\
&\text{(d) } J_2 = \frac{1}{2}\left(D_{11} + D_{22} + \left(D_{11}^2 - 2D_{11}D_{22} + D_{22}^2 + 4D_{12}D_{21}\right)^{(1/2)}\right)
\end{aligned}
\tag{17}
$$

where

$$
\begin{aligned}
D_{11} &= \frac{\bar{B}_{22}t}{Q_1} + \frac{\left(\bar{B}_{21}Q_1 - \bar{B}_{22}Q_2\right)\ln\left(\left(Q_1 + Q_2 e^{a_w t}\right)/\left(Q_1 + Q_2\right)\right)}{Q_1 Q_2 a_w}, \\
D_{12} &= -\frac{\bar{A}_{22}t}{Q_1} - \frac{\left(\bar{A}_{21}Q_1 - \bar{A}_{22}Q_2\right)\ln\left(\left(Q_1 + Q_2 e^{a_w t}\right)/\left(Q_1 + Q_2\right)\right)}{Q_1 Q_2 a_w}, \\
D_{21} &= -\frac{\bar{B}_{12}t}{Q_1} - \frac{\left(\bar{B}_{11}Q_1 - \bar{B}_{12}Q_2\right)\ln\left(\left(Q_1 + Q_2 e^{a_w t}\right)/\left(Q_1 + Q_2\right)\right)}{Q_1 Q_2 a_w}, \\
D_{22} &= \frac{A_{12}t}{Q_1} + \frac{\left(A_{11}Q_1 - A_{12}Q_2\right)\ln\left(\left(Q_1 + Q_2 e^{a_w t}\right)/\left(Q_1 + Q_2\right)\right)}{Q_1 Q_2 a_w}, \\
Q_1 &= \bar{A}_{12}\bar{B}_{22} - \bar{A}_{22}\bar{B}_{12},\ Q_2 = \bar{A}_{11}\bar{B}_{22} + \bar{A}_{12}\bar{B}_{21} - \bar{A}_{21}\bar{B}_{12} - \bar{A}_{22}\bar{B}_{11}
\end{aligned}
$$

Data availability statement

All data, models, and code generated or used during the study appear in the submitted article.

Acknowledgments

This work is supported by the National Key R&D Program of China (Grant Nos. 2017YFE0119500 and 2016YFC0800200), the Projects of International Cooperation and Exchanges NSFC (Grant No. 51620105008), the program of China Scholarships Council (No. 201906320247), the National Natural Science Foundation of China (Grant Nos. 51678319, 51879234 and 51978533), the Natural Science Foundation of Shandong Province (Grant No. ZR2016EEM40), and funding from the European Union's Horizon 2020 research and innovation program Marie Skłodowska–Curie Actions Research and Innovation Staff Exchange (RISE) under grant agreement No. 778360.

Reference

[1]. Bao, S. F., Lou, Y., Dong, Z. L., Mo, H. H., Chen, P. S., & Zhou, R. B., 2014. Causes and countermeasures for vacuum consolidation failure of newly-dredged mud foundation. [In Chinese]. Chinese Journal of Geotechnical Engineering, 36(7), 1350-1359. https://doi.org/10.11779/CJGE201407020.

[2]. Barron R. A., 1948. "Consolidation of fine grained soils by drain wells." Trans of Asce, 113(118),

324-360.

[3]. Basu, D., & Madhav, M. R. 2000. “Effect of prefabricated vertical drain clogging on the rate of consolidation: A numerical study.” Geosynthetics International, 7(3), 189-215. https://doi.org/10.1680/gein.7.0172.

[4]. Bergado, D. T., Manivannan, R., & Balasubramaniam, A. S. 1996. “Filtration criteria for prefabricated vertical drain geotextile filter jackets in soft Bangkok clay.” Geosynthetics International, 3(1), 63-83. https://doi.org/10.1680/gein.3.0054.

[5]. Cao, Y. P., Wang, X. S., Du, L., Ding, J. W., & Deng, Y. F., 2014. “A method of determining nonlinear large strain consolidation parameters of dredged clays.” Water Science and Engineering, 7(2), 218-226. https://doi.org/10.3882/j.issn.1674-2370.2014.02.009.

[6]. Cao, Y., Xu, J., Bian, X., & Xu, G., 2019. “Effect of Clogging on Large Strain Consolidation with Prefabricated Vertical Drains by Vacuum Pressure.” KSCE Journal of Civil Engineering, 23(10), 4190-4200. https://doi.org/10.1007/s12205-019-1884-2.

[7]. Chai, J. C., & Miura, N., 1999. “Investigation of factors affecting vertical drain behavior.” Journal of Geotechnical and Geoenvironmental Engineering, 125(3), 216-226. https://doi.org/10.1061/(ASCE)1090-0241(1999)125:3(216).

[8]. Chai, J., Hong, Z., & Shen, S., 2010. “Vacuum-drain consolidation induced pressure distribution and ground deformation.” Geotextiles and Geomembranes, 28(6), 525-535. https://doi.org/10.1016/j.geotexmem.2010.01.003.

[9]. Chai, J. C., Fu, H. T., Wang, J., & Shen, S. L., 2020. “Behaviour of a PVD unit cell under vacuum pressure and a new method for consolidation analysis.” Computers and Geotechnics, 120, 103415. https://doi.org/10.1016/j.compgeo.2019.103415.

[10]. Cheng, W. Z., Guan Y. F., & Tang T. Z., 2010. “Discussion on treatment technology for land reclamation.” [In Chinese]. Soil Engineering and Foundation, 24(5), 1-3. https://doi.org/10.3969/j.issn.1004-3152.2010.05.001.

[11]. Chu, J., Yan, S. W., & Yang, H., 2000. “Soil improvement by the vacuum preloading method for an oil storage station.” Geotechnique, 50(6), 625-632. https://doi.org/10.1680/geot.2000.50.6.625.

[12]. Deng, Y. B., Xie, K. H., Lu, M. M., Tao, H. B., & Liu, G. B., 2013. “Consolidation by prefabricated vertical drains considering the time dependent well resistance.” Geotextiles and Geomembranes, 36, 20-26. https://doi.org/10.1016/j.geotexmem.2012.10.003.

[13]. Deng, Y. B., Liu, G. B., Indraratna, B., Rujikiatkamjorn, C., & Xie, K. H., 2017. “Model test and theoretical analysis for soft soil foundations improved by prefabricated vertical drains.” International Journal of Geomechanics, 17(1), 04016045. https://doi.org/10.1061/(ASCE)GM.1943-5622.0000711.

[14]. Deng, Y., Liu, L., Cui, Y. J., Feng, Q., Chen, X., & He, N., 2019. “Colloid effect on clogging mechanism of hydraulic reclamation mud improved by vacuum preloading.” Canadian Geotechnical Journal, 56(5), 611-620. https://doi.org/10.1139/cgj-2017-0635.

[15]. Fang, Y., Guo, L., & Huang, J., 2019. “Mechanism test on inhomogeneity of dredged fill during vacuum preloading consolidation.” Marine Georesources & Geotechnology, 37(8), 1007-1017. https://doi.org/10.1080/1064119X.2018.1522398.

[16]. Fu, H., Cai, Y., Wang, J., & Wang, P. 2017. “Experimental study on the combined application of vacuum preloading–variable-spacing electro-osmosis to soft ground improvement.” Geosynthetics International, 24(1), 72-81. https://doi.org/10.1680/jgein.16.00016.

[17]. Geng, X., Indraratna, B., & Rujikiatkamjorn, C., 2012. “Analytical solutions for a single vertical drain with vacuum and time-dependent surcharge preloading in membrane and membraneless systems.”

International Journal of Geomechanics, 12(1), 27-42. https://doi.org/10.1061/(ASCE)GM.1943-5622.0000106.

[18]. Ghosh, C., & Yasuhara, K. 2004. "Clogging and flow characteristics of a geosynthetic drain confined in soils undergoing consolidation." Geosynthetics International, 11(1), 19-34. https://doi.org/10.1680/gein.2004.11.1.19.

[19]. Giroud, J. P. 2005. "Quantification of geosynthetic behavior." Geosynthetics International, 12(1), 2-27. https://doi.org/10.1680/gein.2005.12.1.2.

[20]. Hansbo, S., 1981. "Consolidation of Fine-grained Soils by Prefabricated Drains." Proc., 10th Int. Conf. on Soil Mechanics and Foundation Engineering, Balkema, Rotterdam, vol. 3, 677-682.

[21]. Hong, Z. S., Yin, J., and Cui, Y. J., 2010. Compression behaviour of reconstituted soils at high initial water contents. Géotechnique, 60(9), 691-700. https://doi.org/10.1680/geot.09.P.059.

[22]. Indraratna, B., Bamunawita, C., & Khabbaz, H., 2004. "Numerical modeling of vacuum preloading and field applications." Canadian Geotechnical Journal, 41(6), 1098-1110. https://doi.org/10.1139/t04-054.

[23]. Kim, R., Hong, S. J., Lee, M. J., & Lee, W., 2011. "Time dependent well resistance factor of PVD." Marine Georesources and Geotechnology, 29(2), 131-144. https://doi.org/10.1080/1064119X.2010.525145.

[24]. Kjellman, W., 1952. "Consolidation of clay soils by means of atmospheric pressure." Proceedings of a Conference on Soil Stabilization. Massachusetts Institute of Technology, Boston, 258-263.

[25]. Lei, H., Lu, H., Liu, J., & Zheng, G., 2017. "Experimental Study of the Clogging of Dredger Fills under Vacuum Preloading." International Journal of Geomechanics, 17(12), 04017117.

https://doi.org/10.1061/(ASCE)GM.1943-5622.0001028.

[26]. Lin, D. G., & Chang, K. T. 2009. “Three-dimensional numerical modelling of soft ground improved by prefabricated vertical drains.” Geosynthetics International, 16(5), 339-353. https://doi.org/10.1680/gein.2009.16.5.339.

[27]. Liu, J., Lei, H., Zheng, G., Zhou, H., & Zhang, X., 2017. “Laboratory model study of newly deposited dredger fills using improved multiple-vacuum preloading technique.” Journal of Rock Mechanics and Geotechnical Engineering, 9(5), 924-935. https://doi.org/10.1016/j.jrmge.2017.03.003.

[28]. Miura, N., & Chai, J. C. 2000. “Discharge capacity of prefabricated vertical drains confined in clay.” Geosynthetics International, 7(2), 119-135. https://doi.org/10.1680/gein.7.0169.

[29]. Nguyen, T. T., Indraratna, B., & Rujikiatkamjorn, C., 2016. “An analytical evaluation of radial consolidation with respect to drain degradation.” Faculty of Engineering and Information Sciences - Papers: Part B. 2023.

[30]. Ni, P., Xu, K., Mei, G., & Zhao, Y., 2019. “Effect of vacuum removal on consolidation settlement under a combined vacuum and surcharge preloading.” Geotextiles and Geomembranes, 47(1), 12-22. https://doi.org/10.1016/j.geotexmem.2018.09.004.

[31]. Peng, J., Jiang, R., Tian, Y. M., 2018. “Rigorous Axially Symmetric Consolidation Solution of Vacuum Combined Linear Loading Surcharge Preloading.” Journal of Donghua University (English Edition), 33(04), 279-284. https://doi.org/10.3969/j.issn.1672-5220.2018.04.001.

[32]. Saowapakpiboon, J., Bergado, D. T., Voottipruex, P., Lam, L. G., & Nakakuma, K., 2011. “PVD improvement combined with surcharge and vacuum preloading including simulations.” Geotextiles and Geomembranes, 29(1), 74-82. https://doi.org/10.1016/j.geotexmem.2010.06.008.

[33]. Sharma, J. S., & Xiao, D., 2000. “Characterization of a smear zone around vertical drains by

large-scale laboratory tests." Canadian Geotechnical Journal, 37(6), 1265-1271. https://doi.org/10.1139/t00-050.

[34]. Shen, J., 2018. "Laboratory model test of vacuum preloading on dredged clays at high initial water content." [In Chinese]. Southeast University. https://doi.org/ 10.7666/d.Y2781968.

[35]. Tang, M., & Shang, J. Q., 2000. "Vacuum preloading consolidation of Yaoqiang Airport runway." Geotechnique, 50(6), 613-623. https://doi.org/10.1680/geot.2000.50.6.613.

[36]. Tang, T. Z., Huang, J. Q., Guan, Y. F., Chen, H. B., & Cheng, W. Z., 2010. "Experimental study on dredged fill sludge improved by vacuum preloading." [In Chinese.]. Port and Waterway Engineering, 440, 115–122. https://doi.org/10.3969/j.issn.1002-4972.2010.04.027.

[37]. Tian, Y., Wu, W., Jiang, G., El Naggar, M. H., Mei, G., & Ni, P., 2019. "Analytical solutions for vacuum preloading consolidation with prefabricated vertical drain based on elliptical cylinder model." Computers and Geotechnics, 116, 103202. https://doi.org/10.1016/j.compgeo.2019.103202.

[38]. Venda Oliveira, P. J. 2013. "A formula to predict the effect of the variable discharge capacity of prefabricated vertical drains." Geosynthetics International, 20(6), 408-420. https://doi.org/10.1680/gein.13.00028.

[39]. Wang, J., Cai, Y., Ma, J., Chu, J., Fu, H., Wang, P., & Jin, Y., 2016. "Improved Vacuum Preloading Method for Consolidation of Dredged Clay-Slurry Fill." Journal of Geotechnical and Geoenvironmental Engineering, 142(11), 06016012. https://doi.org/10.1061/(ASCE)GT.1943-5606.0001516.

[40]. Wang, J., Ni, J., Cai, Y., Fu, H., & Wang, P., 2017. "Combination of vacuum preloading and lime treatment for improvement of dredged fill." Engineering Geology, 227, 149-158. https://doi.org/10.1016/j.enggeo.2017.02.013.

[41]. Wang, J., Cai, Y., Fu, H., Hu, X., Cai, Y., Lin, H., & Zheng, W., 2018. “Experimental study on a dredged fill ground improved by a two-stage vacuum preloading method.” Soils and Foundations, 58(3), 766-775. https://doi.org/10.1016/j.sandf.2018.02.028.

[42]. Wang, P., Han, Y., Zhou, Y., Wang, J., Cai, Y., Xu, F., & Pu, H. 2020. “Apparent clogging effect in vacuum-induced consolidation of dredged soil with prefabricated vertical drains.” Geotextiles and Geomembranes. https://doi.org/10.1016/j.geotexmem.2020.02.010.

[43]. Wang, S., Ni, P., Chen, Z., & Mei, G., 2019. “Consolidation solution of soil around a permeable pipe pile.” Marine Georesources & Geotechnology, 1-9. https://doi.org/10.1080/1064119X.2019.1655119.

[44]. Yoshikuni, H., & Nakanodo, H., 1974. “Consolidation of soils by vertical drain wells with finite permeability.” Soils and Foundations, 14(2), 35-46. https://doi.org/10.3208/sandf1972.14.2_35.

[45]. Zeng, L. L., Hong, Z. S., & Cui, Y. J., 2016. “Time-dependent compression behaviour of dredged clays at high water contents in China.” Applied Clay Science, 123, 320-328. https://doi.org/10.1016/j.clay.2016.01.039.

[46]. Zhan, X. J., Lin, W. A., Zhan, L. T., & Chen, Y. M. 2015. “Field implementation of FeCl3-conditioning and vacuum preloading for sewage sludge disposed in a sludge lagoon: a case study.” Geosynthetics International, 22(4), 327-338. https://doi.org/10.1680/gein.15.00015.

[47]. Zhou, Y., & Chai, J. C., 2017. “Equivalent ‘smear’effect due to non-uniform consolidation surrounding a PVD.” Géotechnique, 67(5), 410-419. https://doi.org/10.1680/jgeot.16.P.087.